RSC Advances

PAPER

View Article Online
View Journal | View Issue

Cite this: *RSC Adv.*, 2026, **16**, 4107

Energy from trash: a flexible, facile, and robust triboelectric nanogenerator based on waste polystyrene and application as a human–machine interface

Raj Ankit,[a] Pranav Prakash,[b] Robin Singla[b] and Jayant Kolte *[a]

The accelerated urbanization and rapid growth of the global population has resulted in the generation of massive amounts of municipal solid waste, mainly containing plastics. The improper disposal and minimal recycling rate of these waste materials exacerbate several environmental challenges. The present study focuses on the recycling of waste polystyrene (PS) by fabricating triboelectric nanogenerators (TENGs) based on PS films synthesized by various methods, *i.e.*, solution casting, electrospinning, and spray coating as a positive triboelectric material. Fourier-Transform Infrared (FTIR) spectroscopy and Field-Effect Scanning Electron Microscopy (FE-SEM) were used to analyze the functional groups and morphology of the synthesized films. The spray-coated PS-based TENG exhibited the highest electrical performance with a maximum open circuit voltage (V_{oc}) of 690 V at 4 Hz, short-circuit current of (I_{sc}) of 67 μA at 5 Hz, and maximum output power density of 28 W m^{-2} at 50 MΩ of load resistance. This enhanced performance can be attributed to the nanofibrous nature and increased surface area of the spray-coated films. The practical applications of PS-TENGs were also demonstrated, and include charging various capacitors and powering a calculator using a rectified voltage circuit. Also, the real-time control of a small remote-controlled (RC) car has been successfully demonstrated using PS-based TENGs. This innovative study paves the way for a circular economy by recycling waste plastic material into novel functional materials and accelerates the pathway for energy harvesting and smart sensors.

Received 8th December 2025
Accepted 1st January 2026

DOI: 10.1039/d5ra09473a

rsc.li/rsc-advances

1 Introduction

The rapid growth of the human population is causing urbanization at an alarming rate, resulting in a large amount of waste generation globally. According to a report, municipal solid waste generation is expected to increase from 2.3 billion tonnes in 2023 to 3.8 billion tonnes in 2050.[1] The poor management of these waste materials is adversely affecting the environment in the form of water, soil, and air pollution. Approximately 38 Mt of plastic waste is dumped as garbage, out of which only 6 Mt gets recycled.[2] The packaging industry generates significant amounts of plastic waste, such as polyethylene terephthalate (PET), polystyrene (PS), polypropylene (PP), and polyethylene (PE). The pie chart shown in SI Fig. S1 represents the demand for these plastics globally.[3] Managing plastic garbage is crucial due to its heavy production and ever-increasing demand. The improper treatment of plastic garbage can cause serious environmental and ecological problems. Handling and controlling plastic waste have become extremely important as it generates massive amounts of garbage. To address such issues, a simple yet effective solution has emerged, which is to convert waste into sustainable energy.

One of the promising technologies that has become apparent recently is the triboelectric nanogenerator (TENG), which converts mechanical energy into electrical energy. It has several advantages, including easy fabrication, a simple structure, low cost, and a wide range of material choices. The concept of TENG was first proposed by Wang *et al.* in 2012.[4] The TENG can harvest energy from various sources, such as wind, water waves, raindrops, and human motions.[5–9] Apart from these, the TENGs have become a promising alternative as self-powered sensors for biomedical and environmental monitoring.[10–14]

The triboelectric materials include consumer plastics, also, which are often discarded or thrown into the environment, creating serious environmental pollution. In recent times, several TENGs have been fabricated using waste polymers such as polypropylene (PP),[1,15] polyethylene terephthalate (PET),[16] polyvinyl chloride bags (PVC),[17] polyurethane sponge (PU)[18] *etc.* The PS is significant among other synthetic polymers, also

[a]*Department of Physics and Materials Science, Thapar Institute of Engineering and Technology, Patiala, Punjab, India. E-mail: jayantkolte@thapar.edu; Fax: +91-175-2393020; Tel: +91-175-2393116*

[b]*Department of Electronics and Communication Engineering, Thapar Institute of Engineering and Technology, Patiala, Punjab, India*

known as thermo-col/Styrofoam, and is a common packaging material for consumer products such as disposable food containers[19,20] because it offers very effective thermal insulation and is also permeable to gases and water vapour. Due to its durability, inert nature, and low cost, it is frequently used in several appliances. However, excessive use of PS is a global challenge, and recycling poses a threat to the environment in various ways. The PS may not be the most readily available polymer, but it poses a severe environmental issue because it is heavily used in single-use packaging and is challenging to recycle. It is estimated that around 14 to 15.6 million tonnes of PS are generated each year, and this is expected to increase in the coming year.[21] However, only 10 to 12% of used PS is recycled, leaving the rest to end up in landfills or the environment. This exacerbates plastic pollution and places an additional strain on existing waste management processes. The enormous waste burden necessitates the utilization of waste PS through innovative technologies that can support circular economy and environmental sustainability objectives. The waste PS has garnered little attention in the advancement of TENGs compared to other synthetic polymers, such as PVDF, PTFE, and PDMS. The current study into waste-derived PS-based TENGs for energy harvesting and sensor applications has been driven by these factors.

Waste PS-based TENGs represent an innovative approach for energy harvesting, utilizing recycled PS to convert mechanical energy into electrical energy. Several studies have explored various combinations of materials to enhance the performance of polystyrene-based TENGs. A research group successfully created a recycled polystyrene-ZnO nanocomposite film for use in TENG applications.[22] This film produced twice the output voltage and 4.5 times the power density of non-composite polystyrene TENGs. Adding stearic acid treatment further enhanced the triboelectric performance, demonstrating that this composite could be an effective method for energy collection.[22] Research on electromechanically responsive laminates made from recycled polystyrene has demonstrated that they can generate voltages exceeding 200 V and currents of up to 12 μA in response to movement. These laminates, produced through electrospinning, offer a distinct alternative to traditional ferroelectric materials, demonstrating stability and efficiency in energy conversion.[23] TENGs that can be moved around and made from recycled polystyrene. A portable TENG made from recycled polystyrene and waste corn husk had a power density of 670.5 mW m^{-2}, sufficient to power several small electronic devices and LEDs. This highlights the potential of polystyrene-based TENGs in enabling portable and cost-effective energy solutions.[24]

These studies demonstrate how waste PS can be utilized in TENG applications. However, we must also consider the broader context of waste management and energy sustainability. The integration of waste materials for energy harvesting technologies not only reduces environmental pollution significantly but also promotes the development of green energy solutions. On the other hand, to fully utilize these potentials in real-world situations, problems such as cost-effectiveness, scalability, and long-term durability must be addressed, as the utilization of waste PS for developing self-powered sensors, energy harvesting devices, and optimizing their performance is still in its early stages.

The three key stages involved in electricity generation *via* friction in TENGs are charge generation, charge dissipation, and charge transfer. However, the optimization and enhancement of electrical output performance are still crucial. Most reports focus on enhancing charge generation through chemical modifications. This work focuses on the scalable synthesis of waste PS, the utilization of waste PS, and the effect of an increase in surface area on the fabrication of TENG. To achieve this, waste PS is collected from local waste sites. The PS film has been synthesized using solution casting, electrospinning, and spray coating methods. This work shows the potential for reducing energy costs and waste management.

2 Experimental

2.1 Materials

Waste PS was obtained from discarded packaging debris, and chloroform (99%) was purchased from Loba Chemie Pvt. Ltd, deionized water (DI) was purchased from Organo Biotech Laboratories Pvt. Ltd. Conductive copper tape of 3M, and fluorinated propylene copolymer (FEP) were procured from Amazon.

2.2 Solution preparation

In the first step, waste PS was washed several times using DI water and left to dry at room temperature. Then, a 10 wt% solution of waste PS was prepared by dissolving waste PS in chloroform in a 50 ml beaker.

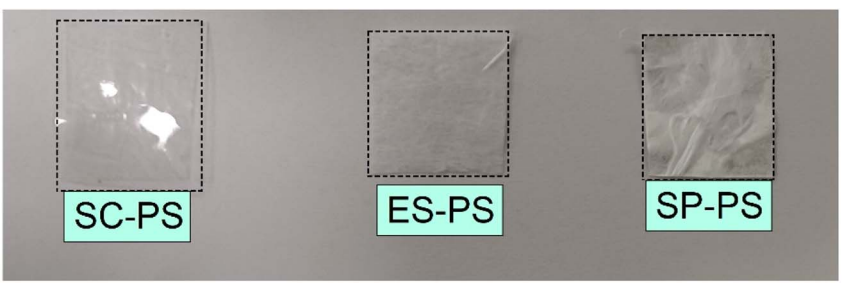

Fig. 1 Pictures of fabricated samples.

2.3 Preparation of polystyrene films by different methods

The waste PS film has been synthesized by three methods: (i) solution casting, (ii) electrospinning, and (iii) spray coating. The image of all the fabricated samples is shown in Fig. 1.

In the solution casting method, the waste PS solution was poured into a Petri dish and left to dry at room temperature. Once the solution dried, it was peeled off from the glass Petri dish. This sample was labelled as SC-PS.

The electrospinning of the solution was done using standard electrospinning equipment procured from ESPIN-NANO (Chennai), India. A stainless-steel needle (21 gauge) coupled with a 10 ml solution containing a syringe pump was used. During the process, the flow rate of 1 ml h^{-1}, the needle-to-collector distance of 12 cm, and a high voltage supply of 12 KV were adjusted. Fibers were collected on a stainless-steel drum wrapped with aluminium foil and ground. This sample was labelled as ES-PS.

For the spray-coated film, the solution was spray-coated on an aluminum foil using a Pilot Power AB-05 airbrush gun. The diameter of the nozzle was 0.5 mm. The PS solution was poured into the cup of the gun and sprayed at an angle of 45° from a distance of 15 cm. A very fine layer of fibrous film of waste PS uniformly gets coated on an aluminum foil. This sample was labelled as SP-PS.

2.4 Fabrication of various PS-TENGs

A 2 × 2 cm^2 of synthesized waste SC-PS film, cut and 3M copper tape was used as an electrode, while 2 × 2 cm^2 of synthesized waste PS fibrous film (ES-PS, SP-PS), coupled with aluminum foil, was cut out. The commercially available FEP film of 2 × 2 cm^2 with copper tape was utilized as a negative triboelectric counterpart, forming the TENG based on PS and FEP triboelectric pairs. The TENGs have been further utilized in energy harvesting and sensor applications.

2.5 Characterizations

A field-effect scanning electron microscope (FE-SEM; Carl Zeiss Sigma 500) was used to study the morphology of the synthesized fibers. To understand the functional groups and bonding structure of waste PS samples, Fourier-transform infrared (FTIR) spectroscopy (PerkinElmer Spectrum IT-FTIR, from 500 to 4000 cm^{-1}) was used. Two different materials with an active area of 2 × 2 cm^2 were fixed at the two terminals of a standard linear motor-based testing system for the contact-separation process. The open-circuit voltage was measured by a digital oscilloscope (SIGLENT SDS1104X-E, impedance = 1 MΩ), and the short-circuit current of TENG was measured by an electrometer (Keithley 6517B). All the electric measurements were recorded at room temperature.

3 Results and discussions

3.1 FTIR analysis

FTIR has been used to analyze different functional groups and chemical compositions of the PS films synthesized by different methods. Fig. 2 depicts the FTIR spectra of PS films recorded in the range of 3500–600 cm^{-1}. All the characteristic peaks associated with PS were present in the FTIR spectra of three films, SC-PS, ES-PS, and SP-PS, confirming the preservation of its chemical composition regardless of synthesis methods.

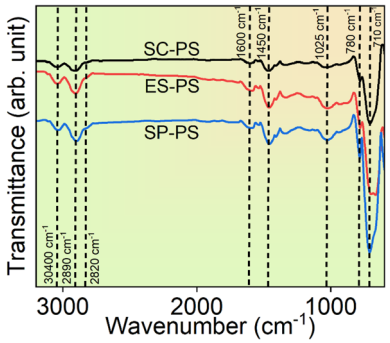

Fig. 2 FTIR spectra of spray-coated (SC-PS), electrospun (ES-PS), and solution-casted (SP-PS) fabricated films.

The peak at 3040 cm^{-1} corresponds to aromatic =C–H stretching vibration, while peaks at 2890 cm^{-1} and 2820 cm^{-1} show the symmetric and asymmetric stretching of $-CH_2-$ respectively. The transmission peaks at 1600 and 1450 cm^{-1} attributed to aromatic C=C stretching. Further, the peak at 1025 cm^{-1} can be identified as in plane =C–H deformation while the peak at 780 cm^{-1} can be identified as out of plane = C–H deformation. The band at 710 cm^{-1} corresponds to out-of-plane aromatic deformation. Similar observations were reported by other researchers.[25,26]

3.2 Morphological analysis

Typically, the surface area and surface roughness of a triboelectric material play an important role in increasing the output performance of the TENGs. So, to examine the effect of surface area and surface roughness on the performance of TENG, the morphology of the PS film has been studied and the electrical performance of TENGs is correlated to it.

Fig. 3 represents the SEM images of the films. The surface morphological difference between the SC-PS, ES-PS, and SP-PS is substantial and can be observed from the SEM images. The average diameter of ES-PS fibers is approximately 14.4 μm with a standard deviation (SD) of 8.58 μm, having very high porosity (average pore size of 0.07 μm and SD of 0.03 μm) in each fiber, and the average diameter of fibers of SP-PS is about 377 nm with SD of 18 nm, having a much higher density of fibers compared to ES-PS. In contrast, no porosity and roughness is observed in SC-PS. The smaller diameter of SP-PS fibers compared to ES-PS fibers can be attributed to the properties of the materials and processing techniques. The spray coating controls the production of fiber more precisely, resulting in reduced diameters. This method atomizes a polymeric solution using high-velocity air, creating smaller droplets that solidify into very fine fibers. On the other hand, the electrospinning depends on the viscosity of the solution, concentration of the solution, and electrical forces, which result in thicker fibers. The increase in ionic conductivity can result in smaller fiber diameters, as evidenced

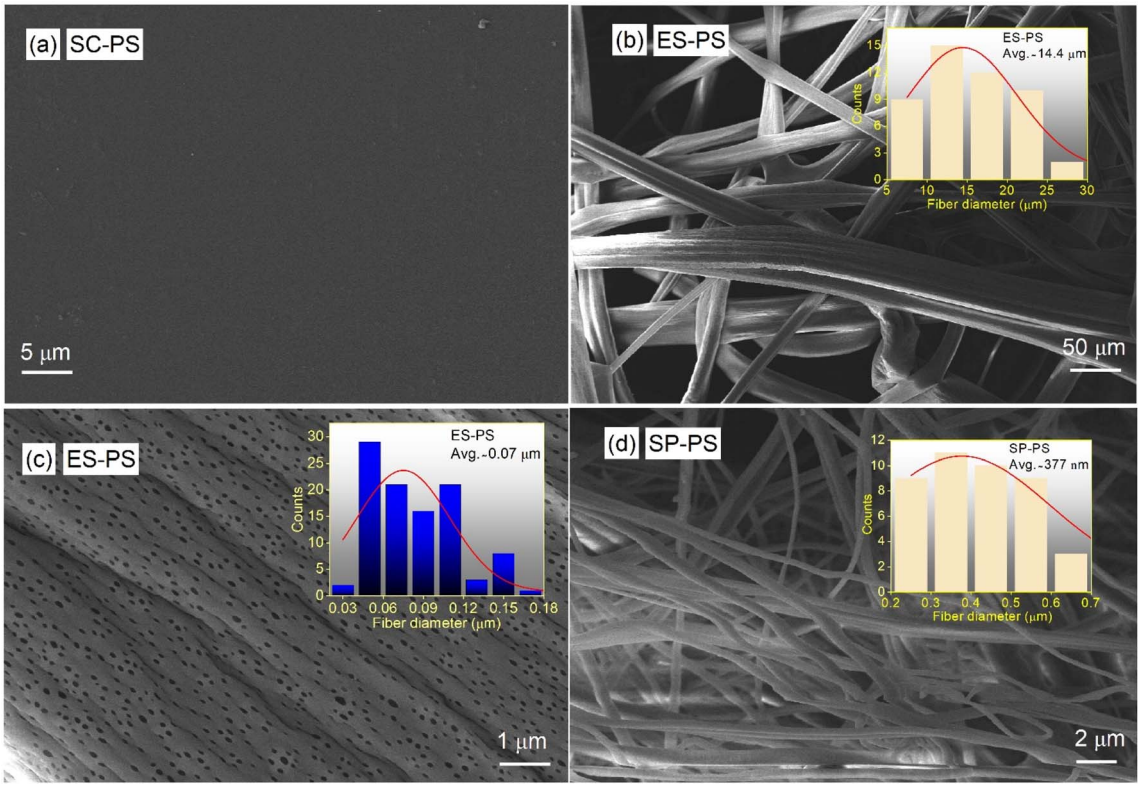

Fig. 3 SEM images of (a) solution casted (SC-PS), (b and c) electrospun (ES-PS), and histogram showing fiber analysis and pore size analysis, (d) spray-coated (SP-PS), and histogram showing fiber analysis of synthesized film.

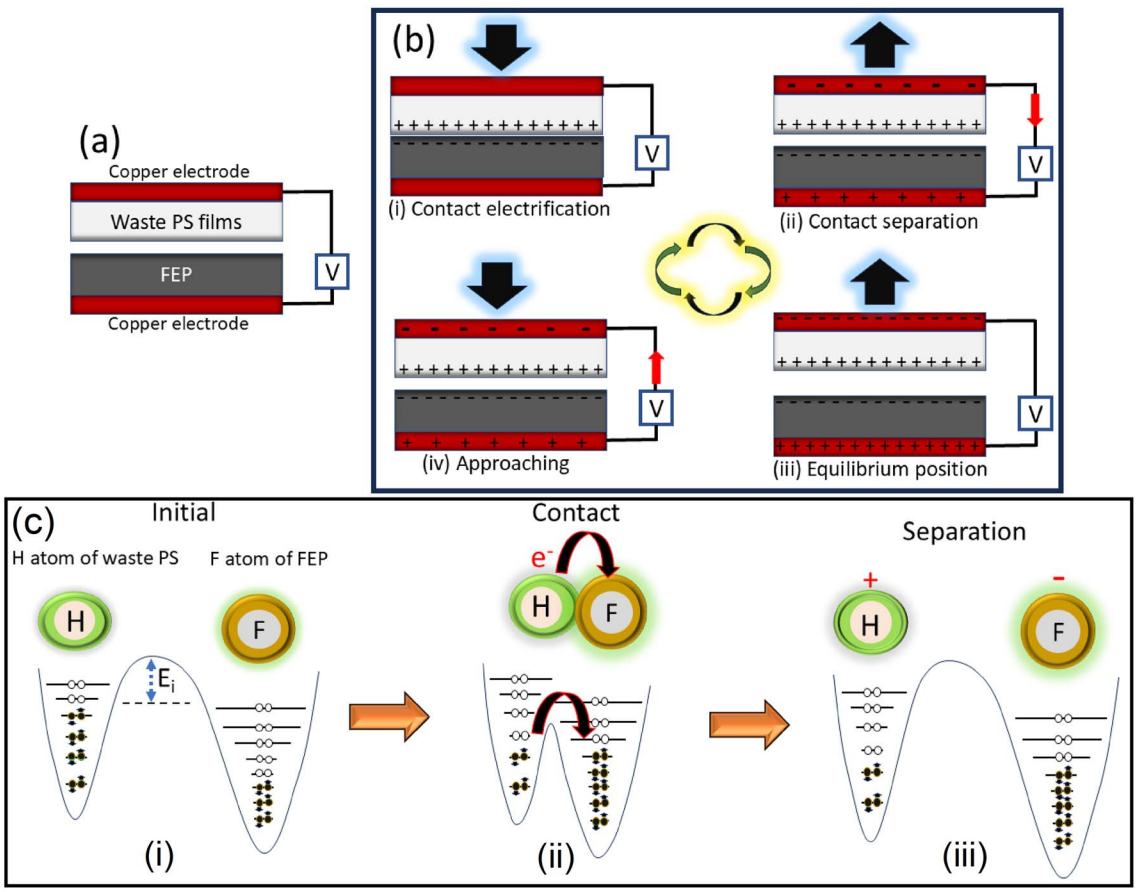

Fig. 4 (a and b) Working mechanism and (c)(i–iii) electron cloud model describing contact-electrification in PS-TENG.

by a study relating conductivity to jet radius.[27] However, spray coating is independent of these parameters, facilitating the fabrication of finer fibers.

3.3 Working mechanism and electron cloud model of PS-based TENGs

The working mechanism of PS-based TENGs is shown in Fig. 4. When the top and bottom layers come into contact, an external force is exerted on the TENGs, and the transfer of surface charge occurs due to contact electrification. The PS-based films act as a positive triboelectric material, while FEP is a negative triboelectric material. So, PS will lose electrons while FEP will gain electrons. Due to this, the positive charges accumulate on the surface of PS films while negative charges generated on the surface of FEP film (Fig. 4b(i)). When the layers get separated because of an external force, the potential difference develops as shown in Fig. 4b(ii). As the separation gap increases, the potential difference also increases until equilibrium is reached (Fig. 4b(iii)). Due to electrostatic induction, the opposite charge will be induced on the corresponding electrodes of the films, and the electrons will start flowing through the closed circuit of electrodes (Fig. 4b(iv)). A mechanism has been proposed by Wang and coworkers[28] to explain the transfer of electrons at the atomic–level interactions using an electron cloud model. The possible mechanism of electron transfer due to contact electrification is illustrated in Fig. 4c. At the initial stage, when PS and FEP are separated, the H atoms of PS and the F atoms of FEP remain isolated, with no overlapping of their respective electron clouds (Fig. 4c(i)). Since the interfacial potential barrier (E_i) prohibits electron transfer between the clouds, electrons remain intact inside the atoms in the potential well. When the PS and FEP come in contact with each other, at the interface as soon as the interatomic distance enters a repulsive region, the electron clouds overlap, reducing the interfacial potential barrier as depicted in Fig. 4c(ii). This reduction allows electron transfer between the PS and FEP polymer interface.

Once the layers are separated, the surface of PS becomes positively charged while the surface of FEP becomes negatively charged (Fig. 4c(iii)). With the repetitive contact separation cycle, the continuous potential is generated between the electrodes, which promotes charge flow and generates current in the external circuit.

3.4 Testing of electrical outputs

The waste PS-based PS-TENGs have been tested for open circuit voltage and short circuit current at different frequencies, *i.e.*, 3 Hz, 4 Hz, and 5 Hz, under a constant force of 3 N. The output power density of PS-TENG depends on both V_{oc} and I_{sc} values at different load resistances. So, the power density is obtained using both the voltage and current values obtained at different load resistances, divided by the area of the samples used in PS-TENGs. Fig. 5 shows the electrical outputs of TENGs-based SC-PS, ES-PS, and SP-PS as positive triboelectric material, while FEP is a negative triboelectric material.

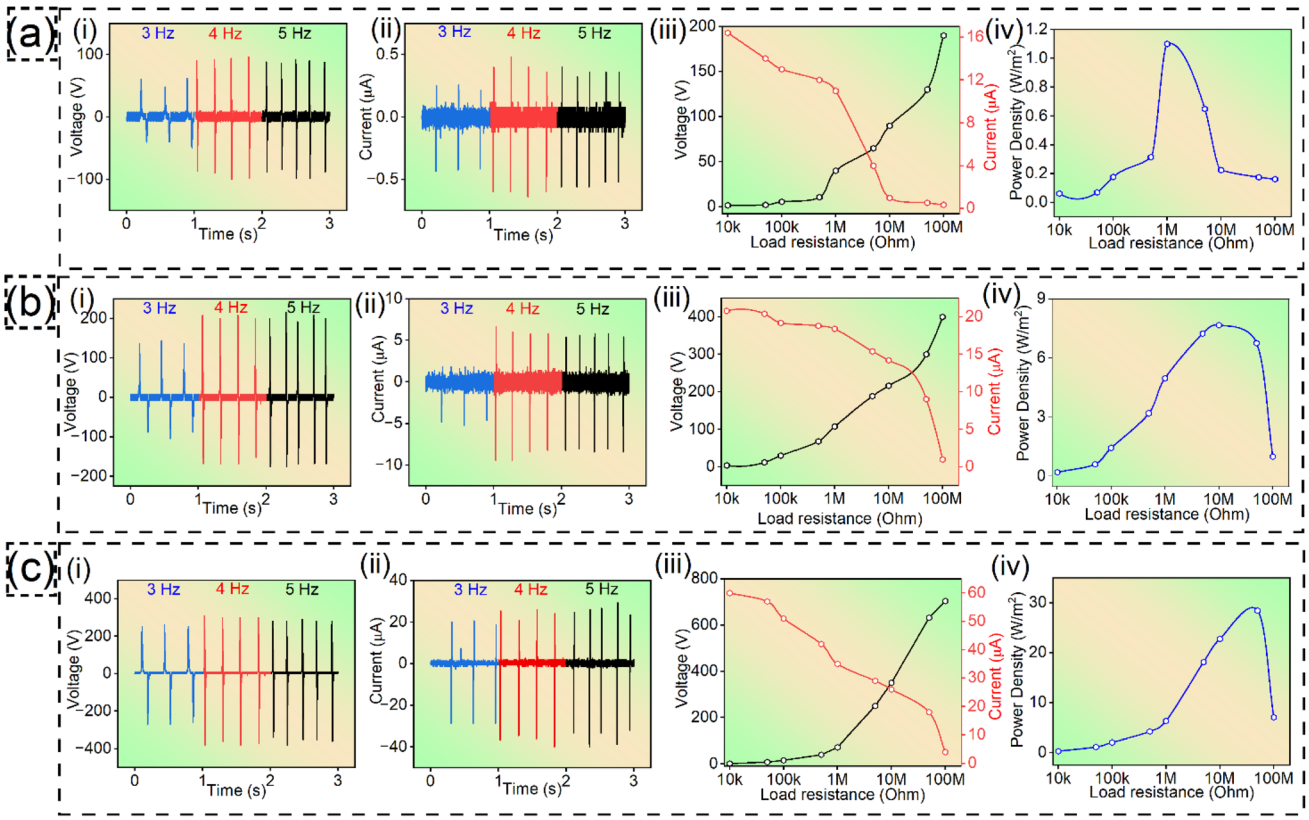

Fig. 5 (i) Open-circuit voltage (V_{oc}), (ii) short-circuit current (I_{sc}), (iii) V_{oc} and I_{sc} with load resistance, and (iv) power-density with load resistance, for (a) SC-PS, (b) ES-PS, and (c) SP-PS, respectively.

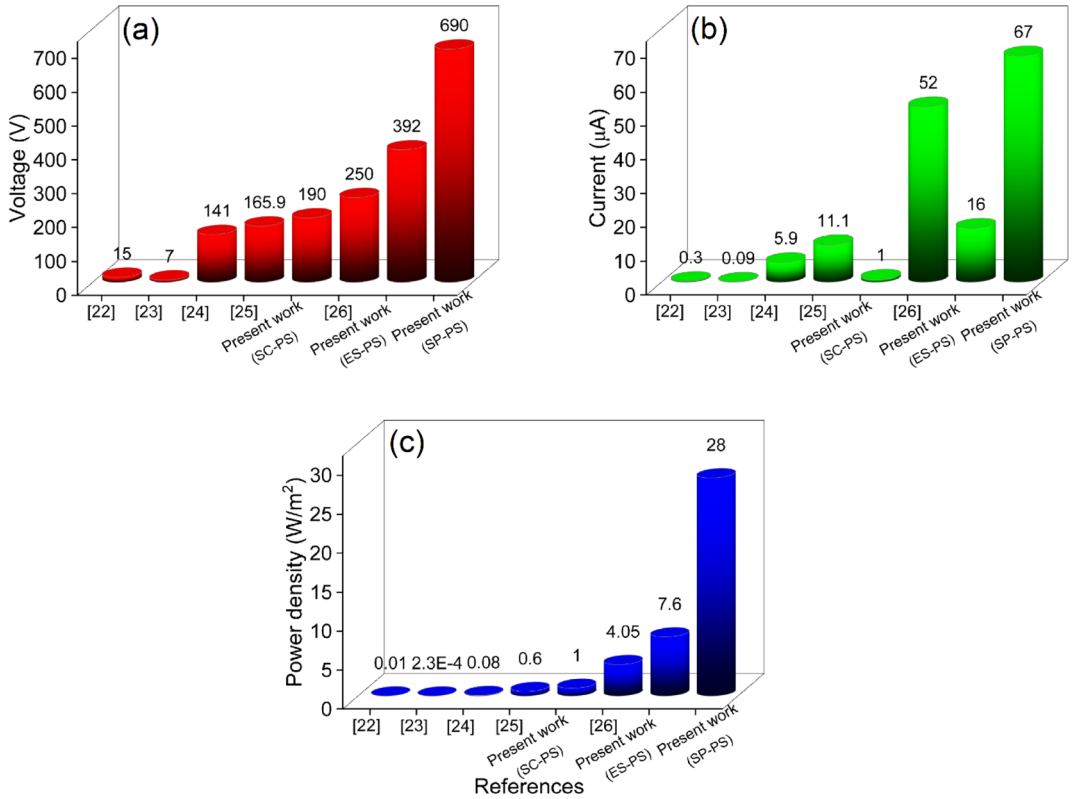

Fig. 6 Triboelectric outputs (a) open-circuit voltage, (b) short-circuit current, and (c) power density reported in the literature[29–33] compared with the present study.

It can be observed that PS-TENG based on SC-PS shows a maximum V_{oc} of 190 V and I_{sc} of 1 μA at a frequency of 4 Hz. The TENG shows a maximum output power density of 1 W m^{-2} at 1 MΩ of load resistance. The ES-PS-based TENG shows a maximum V_{oc} of 392 V at 5 Hz, I_{sc} of 16 μA at 4 Hz, and output power density of 7.6 W m^{-2} at 10 MΩ of load resistance. Similarly, SP-PS-based TENG shows a maximum V_{oc} of 690 V at 4 Hz, I_{sc} of 67 μA at 5 Hz, and a maximum output power density of 28 W m^{-2} at 50 MΩ of load resistance. The SI Fig. S2 represents the average and SD of V_{oc} and I_{sc}. All the readings were taken under 3 N of mechanical stimulation measured using a load cell. Fig. 6 shows a comparative analysis of available literature based on polystyrene-based TENGs. It can be observed that SP-PS-based TENG shows 28 times more power output than SC-PS-based TENG due to the enhancement in surface charge generation due to the increase in surface area.

The Fig. 6 highlights that the present work, using fibrous films, shows the maximum power density amongst the reported results. The enhanced electrical output characteristics can be attributed to the unique morphology of fibrous films. TENG based on SP-PS shows the highest output density because of the denser and nanometer-sized fibers. So, the result concludes that the increase in surface area yields higher electrical output.

3.5 PS-TENG as a power source

Since the TENGs generate alternating signals, which are unsuitable for powering wearable and portable electronic devices, a full bridge rectifier circuit has been utilized to charge capacitors. Further, the charged capacitors can be utilized to power portable electronics. The equivalent circuit of PS-TENG for charging capacitors and powering electronic devices through the rectifier circuit is shown in Fig. 7a.

Different capacitors are charged using the rectified voltage of the SC-PS-based TENG, and the voltage accumulated across the capacitors is shown in Fig. 7b. Further, two 47 μF capacitors were connected in series such that the resultant capacitance is 23.5 μF, and are used for powering the calculator (Fig. 7c and d).

3.6 Toy car controller using contact-separation-based PS-TENG as human–machine interface

In the current era, Internet-of-things (IoT) based devices have a significant impact on both personal electronics and industrial applications. Researchers have predicted that in the upcoming years, the number of IoT devices will grow exponentially.[34] Recently, self-powered wearable flexible devices have gained significant attention for resolving the increasing energy crisis and enabling battery-free applications. The TENG has emerged as a promising energy harvesting technology offering various benefits, such as a wide range of materials and self-powered signals that can be used for battery-free systems and wearable electronics. Therefore, extensive research efforts have been initiated, leading to advancements in various domains like self-powered sensors,[35] actuators,[11] and energy harvesters.[36,37]

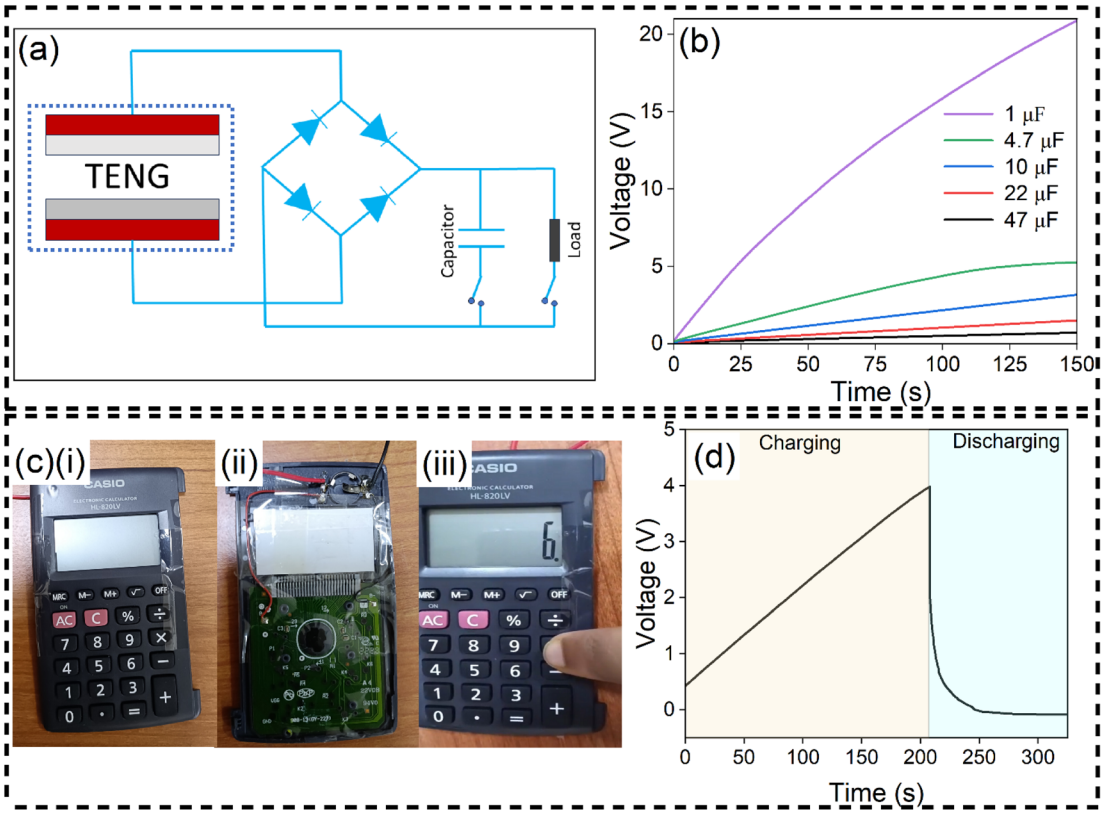

Fig. 7 (a) Equivalent circuit of the bridge rectifier for converting the TENG into a direct current signal for powering electronic equipment with the help of capacitors, (b) voltage accumulated across the capacitors. Photograph of (c)(i) calculator in switch off mode, (ii) calculator without battery, (iii) calculator in switch on mode with the help of TENG and charged capacitor, (d) charging and discharging of 23.5 μF capacitors for powering the calculator.

The control interface is a crucial fundamental component that facilitates the interaction between humans and machines. With the advancement in TENGs globally, the control interface based on triboelectricity has become significantly appealing as it offers unique advantages such as flexibility, low cost, high performance, and self-generated signals.

A contact-separation mode-based triboelectric control system for multidirectional sensing and toy car control has been developed. The real-time control of a small remote-controlled (RC) car is successfully demonstrated using SP-PS-based TENG. The triboelectric control system consists of four arch-shaped PS-TENG using SP-PS as positive triboelectric material and FEP as negative triboelectric material, coupled with aluminium and copper electrodes, respectively. The TENG sensors marked as ⬆, ➡, ⬇, and ⬅ as a game controller are shown in Fig. 8. The block diagram and the photograph of the entire control system, having wireless communication systems, are shown in Fig. 8b and c. The whole setup consists of a wireless RC car controlled by four TENG-based sensors, two Arduino Uno microcontrollers, a 433 MHz radio frequency transmitter and receiver, an L298 motor driver, and a motor circuit. The voltage signal from the TENG sensors is converted into a digital signal by Arduino for accurate processing. The microcontroller encodes such that the signals are transmitted wirelessly to the receiver using an RF transmitter. The decoded signals are then received by the microcontroller through the RF receiver and transmitted to the motor driver. The motor driver helps in the efficient control of the motors. The real-time video

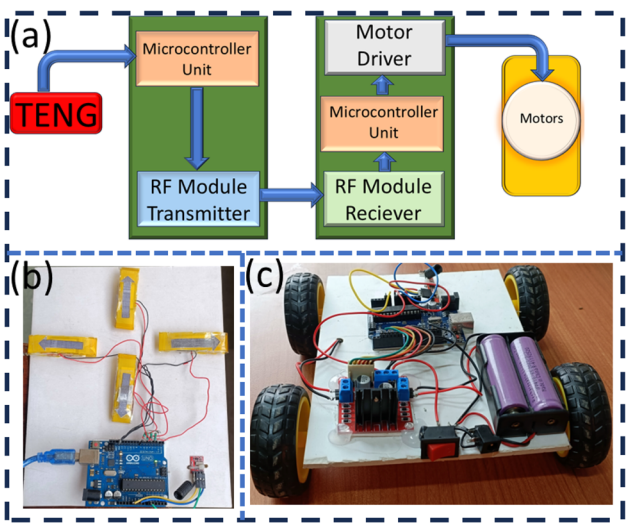

Fig. 8 (a) Block diagram of wireless control system, (b) wireless controlling using TENG used as switches with microcontroller and RF module transmitter, and (c) toy car with RF module receiver and microcontroller connected with motor driver.

demonstration of the wireless remote-controlled car can be found in the SI Video V1. This demonstration of the triboelectric control system shows the promising potential for diverse applications in the human–machine interface, inspiring more research and applications.

4 Conclusions

The study focuses on the innovative approach of recycling plastic waste by fabricating TENGs based on discarded waste polystyrene. The fabricated PS-based functional films demonstrated excellent triboelectric performance, with spray-coated films exhibiting the highest output power density due to increased surface area and dense nanostructured morphology. These results illustrate the paramount role of surface characteristics for enhancing the TENG performance. The practical applications of PS-TENGs, from self-powered devices to human–machine interface and energy harvesting applications, pave a promising pathway toward sustainable waste management and energy solutions. By addressing environmental challenges and enhancing energy efficiency, this study establishes a foundation for innovations in energy harvesting technologies and self-powered sensors utilizing waste materials.

Author contributions

Raj Ankit: conceptualization, visualization, synthesis, methodology, characterization, analysis, validation, writing – original draft, review, and editing. Pranav Prakash: software, methodology, visualization, analysis, writing – review and editing. Robin Singla: conceptualization, supervision, investigation. Jayant Kolte: conceptualization, supervision, investigation, methodology, validation, writing – review and editing.

Conflicts of interest

The authors declare that they have no known competing financial interests or personal relationships that could have appeared to influence the work reported in this paper.

Data availability

Data will be made available on request.

Supplementary information (SI) is available. See DOI: https://doi.org/10.1039/d5ra09473a.

Acknowledgements

The authors thank DST FIST (grant no. SR/FST/PS-II/2018/53) for providing characterization facilities.

References

1 G. Khandelwal, *et al.*, Trash to energy: a facile, robust and cheap approach for mitigating environment pollutant using household triboelectric nanogenerator, *Appl. Energy*, 2018, **219**, 338–349.
2 S. S. V. Vuppaladadiyam, *et al.*, Waste to energy: Trending key challenges and current technologies in waste plastic management, *Sci. Total Environ.*, 2023, 169436.
3 J. Yu, *et al.*, Thermal degradation of PVC: A review, *Waste Manag.*, 2016, **48**, 300–314.
4 F.-R. Fan, Z.-Q. Tian and Z. L. Wang, Flexible triboelectric generator, *Nano energy*, 2012, **1**(2), 328–334.
5 S. Wang, *et al.*, Efficient scavenging of solar and wind energies in a smart city, *ACS Nano*, 2016, **10**(6), 5696–5700.
6 G. Yang, *et al.*, Ag Interconnects Enhanced Polydimethylsiloxane Microstructure for Self-Recovery Fluid Pipe Energy Harvester, *Macromol. Mater. Eng.*, 2021, **306**(4), 2000666.
7 J. Nie, *et al.*, Power generation from the interaction of a liquid droplet and a liquid membrane, *Nat. Commun.*, 2019, **10**(1), 2264.
8 Y. Fu, *et al.*, Self-powered, stretchable, fiber-based electronic-skin for actively detecting human motion and environmental atmosphere based on a triboelectrification/gas-sensing coupling effect, *J. Mater. Chem. C*, 2017, **5**(5), 1231–1239.
9 H. Chen, *et al.*, Highly extendable triboelectric nanogenerators with sustainable electrical output for deployable multifunctional metamaterials, *Nano Energy*, 2025, 111563.
10 H. Zhang, *et al.*, Triboelectric nanogenerator as self-powered active sensors for detecting liquid/gaseous water/ethanol, *Nano Energy*, 2013, **2**(5), 693–701.
11 Z. H. Lin, *et al.*, A self-powered triboelectric nanosensor for mercury ion detection, *Angew. Chem.*, 2013, **125**(19), 5065–5069.
12 J. Yang, *et al.*, Eardrum-inspired active sensors for self-powered cardiovascular system characterization and throat-attached anti-interference voice recognition, *Adv. Mater.*, 2015, **27**(8), 1316–1326.
13 H. Chen, *et al.*, Multifunctional triboelectric metamaterials with unidirectional charge transfer channels for linear mechanical motion energy harvesting, *Adv. Funct. Mater.*, 2025, **35**(10), 2416749.
14 H. Chen, J. Shi and A. Akbarzadeh, Curved Architected Triboelectric Metamaterials: Auxeticity-Enabled Enhanced Figure-of-Merit, *Adv. Funct. Mater.*, 2023, **33**(49), 2306022.
15 H. Varghese and A. Chandran, Triboelectric nanogenerator from used surgical face mask and waste mylar materials aiding the circular economy, *ACS Appl. Mater. Interfaces*, 2021, **13**(43), 51132–51140.
16 M. Sahu, *et al.*, Additive manufacturing-based recycling of laboratory waste into energy harvesting device for self-powered applications, *Nano Energy*, 2021, **88**, 106255.
17 X. Feng, Q. Li and K. Wang, Waste plastic triboelectric nanogenerators using recycled plastic bags for power generation, *ACS Appl. Mater. Interfaces*, 2020, **13**(1), 400–410.
18 H. Zhang, *et al.*, Progressive contact-separate triboelectric nanogenerator based on conductive polyurethane foam regulated with a Bennet doubler conditioning circuit, *Nano energy*, 2018, **51**, 10–18.
19 A. N. Uttaravalli, S. Dinda and B. R. Gidla, Scientific and engineering aspects of potential applications of post-

consumer (waste) expanded polystyrene: a review, *Process Saf. Environ. Prot.*, 2020, **137**, 140–148.

20 M. Ryberg, A. Laurent and M. Z. Hauschild, *Mapping of global plastic value chain and plastic losses to the environment: with a particular focus on marine environment*, UN Environment Programme, 2018, https://www.unep.org/resources/report/mapping-global-plastics-value-chain-and-plastics-losses-environment-particular, accessed on 14th November 2025.

21 D. Tkalčić, *et al.*, Performance Assessment of Mechanically Recycled EPS, *Materials*, 2025, **18**(19), 4547.

22 D. Kamaruzaman, *et al.*, Polystyrene Waste-ZnO nanocomposite film for energy harvesting *via* hydrophobic triboelectric nanogenerator: Transforming waste into energy, *Mater. Today Sustain.*, 2024, **26**, 100726.

23 A. Šutka, *et al.*, Recycled Polystyrene Waste to Triboelectric Nanogenerators: Volumetric Electromechanically Responsive Laminates from Same-Material Contact Electrification, *Adv. Energy Sustain. Res.*, 2024, **5**(6), 2300259.

24 E. A. Elvira-Hernandez, *et al.*, Green energy harvesting to power electronic devices using portable triboelectric nanogenerator based on waste corn husk and recycled polystyrene, *Energy Rep.*, 2024, **11**, 276–286.

25 M. F. H. Al-Kadhemy, Z. S. Rasheed and S. R. Salim, Fourier transform infrared spectroscopy for irradiation coumarin doped polystyrene polymer films by alpha ray, *J. Radiat. Res. Appl. Sci.*, 2016, **9**(3), 321–331.

26 D. Olmos, E. Martín and J. González-Benito, New molecular-scale information on polystyrene dynamics in PS and PS–BaTiO 3 composites from FTIR spectroscopy, *Phys. Chem. Chem. Phys.*, 2014, **16**(44), 24339–24349.

27 C. Shin and G. G. Chase, Nanofibers from recycle waste expanded polystyrene using natural solvent, *Polym. Bull.*, 2005, **55**(3), 209–215.

28 S. Lin, *et al.*, The overlapped electron-cloud model for electron transfer in contact electrification, *Adv. Funct. Mater.*, 2020, **30**(11), 1909724.

29 J. Park, *et al.*, Electrospun nanofiber covered polystyrene micro-nano hybrid structures for triboelectric nanogenerator and supercapacitor, *Micromachines*, 2022, **13**(3), 380.

30 A. K. Gupta, *et al.*, ZnO-polystyrene composite as efficient energy harvest for self-powered triboelectric nanogenerator, *ECS J. Solid State Sci. Technol.*, 2020, **9**(11), 115019.

31 M. Wu, A drum structure triboelectric nanogenerator based on PS/MXene for football training monitoring, *AIP Adv.*, 2023, **13**(8), 085012.

32 C. Luo, *et al.*, Preparation and application of high performance PVDF/PS electrospinning film-based triboelectric nanogenerator, *Chem. Phys. Lett.*, 2023, **813**, 140276.

33 S. M. Nawaz, *et al.*, Energy-from-waste: A triboelectric nanogenerator fabricated from waste polystyrene for energy harvesting and self-powered sensor, *Nano Energy*, 2022, **104**, 107902.

34 A. Nordrum, Popular internet of things forecast of 50 billion devices by 2020 is outdated, *IEEE spectrum*, 2016, **18**(3), 223–236.

35 Y. Yang, *et al.*, A single-electrode based triboelectric nanogenerator as self-powered tracking system, *Adv. Mater.*, 2013, **25**(45), 6594–6601.

36 H.-J. Yoon, H. Ryu and S.-W. Kim, Sustainable powering triboelectric nanogenerators: Approaches and the path towards efficient use, *Nano Energy*, 2018, **51**, 270–285.

37 C. Zhao, *et al.*, Hybrid piezo/triboelectric nanogenerator for highly efficient and stable rotation energy harvesting, *Nano Energy*, 2019, **57**, 440–449.